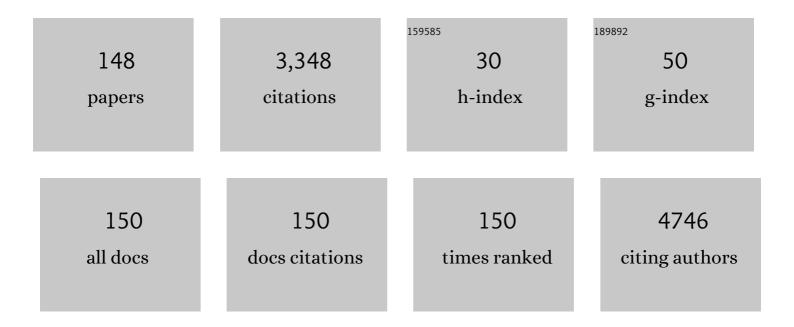
List of Publications by Year in descending order

Source: https://exaly.com/author-pdf/5192998/publications.pdf Version: 2024-02-01



DANIELA MANNO

#	Article	IF	CITATIONS
1	A new amperometric nanostructured sensor for the analytical determination of hydrogen peroxide. Biosensors and Bioelectronics, 2008, 24, 1057-1063.	10.1	197
2	WO3 gas sensors prepared by thermal oxidization of tungsten. Sensors and Actuators B: Chemical, 2008, 133, 321-326.	7.8	175
3	Poly(vinyl alcohol) capped silver nanoparticles as localized surface plasmon resonance-based hydrogen peroxide sensor. Sensors and Actuators B: Chemical, 2009, 138, 625-630.	7.8	167
4	Size-dependent lattice contraction inCdS1â^'xSexnanocrystals embedded in glass observed by Raman scattering. Physical Review B, 1992, 45, 13792-13795.	3.2	136
5	Green synthesis of silver nanoparticles with sucrose and maltose: Morphological and structural characterization. Journal of Non-Crystalline Solids, 2010, 356, 344-350.	3.1	118
6	Physical and structural characterization of tungsten oxide thin films for NO gas detection. Thin Solid Films, 1998, 324, 44-51.	1.8	94
7	Green synthesis of sucralose-capped silver nanoparticles for fast colorimetric triethylamine detection. Sensors and Actuators B: Chemical, 2013, 178, 1-9.	7.8	88
8	Characterization of African dust over southern Italy. Atmospheric Chemistry and Physics, 2003, 3, 2147-2159.	4.9	81
9	Synthesis and characterization of ZnS nanoparticles in water/AOT/n-heptane microemulsions. Applied Physics A: Materials Science and Processing, 1999, 69, 369-373.	2.3	70
10	Synthesis and characterization of starch-stabilized Ag nanostructures for sensors applications. Journal of Non-Crystalline Solids, 2008, 354, 5515-5520.	3.1	70
11	Aligning Singleâ€Walled Carbon Nanotubes By Means Of Langmuir–Blodgett Film Deposition: Optical, Morphological, and Photoâ€electrochemical Studies. Advanced Functional Materials, 2010, 20, 2481-2488.	14.9	70
12	Titanium oxide thin films for NH3 monitoring: Structural and physical characterizations. Journal of Applied Physics, 1997, 82, 54-59.	2.5	69
13	Highly selective hydrogenation of quinolines promoted by recyclable polymer supported palladium nanoparticles under mild conditions in aqueous medium. Applied Catalysis A: General, 2014, 481, 89-95.	4.3	64
14	Structural and electrical properties of sputtered vanadium oxide thin films for applications as gas sensing material. Journal of Applied Physics, 1997, 81, 2709-2714.	2.5	56
15	Non-functionalized silver nanoparticles for a localized surface plasmon resonance-based glucose sensor. Nanotechnology, 2009, 20, 165501.	2.6	56
16	Porphyrin Dimers Linked by a Conjugated Alkyne Bridge:  Novel Moieties for the Growth of Langmuirâ^'Blodgett Films and Their Applications in Gas Sensors. Langmuir, 1997, 13, 5951-5956.	3.5	49
17	Effects of thermal annealing on optical absorption of amorphous indium selenide thin films. Solar Energy Materials and Solar Cells, 1987, 15, 209-218.	0.4	44
18	Kinetic behavior analysis of porphyrin Langmuir–Blodgett films for conductive gas sensors. Journal of Applied Physics, 1998, 84, 1416-1420.	2.5	44

#	Article	IF	CITATIONS
19	Gas-sensing properties of sputtered thin films of tungsten oxide. Journal Physics D: Applied Physics, 1997, 30, 3211-3215.	2.8	42
20	Gas-sensing properties of porphyrin dimer Langmuir–Blodgett films. Thin Solid Films, 1998, 327-329, 341-344.	1.8	41
21	Enhanced electrical conductivity of collagen films through long-range aligned iron oxide nanoparticles. Journal of Colloid and Interface Science, 2017, 501, 185-191.	9.4	40
22	Aligned arrays of carbon nanotubes: modulation of orientation and selected-area growth. Chemical Physics Letters, 2003, 367, 109-115.	2.6	39
23	The influence of inulin addition on the morphological and structural properties of durum wheat pasta. International Journal of Food Science and Technology, 2009, 44, 2218-2224.	2.7	36
24	Structural and electrical properties of In2O3–SeO2 mixed oxide thin films for gas sensing applications. Journal of Applied Physics, 2000, 88, 6571-6577.	2.5	35
25	Atomic force acoustic microscopy characterization of nanostructured selenium–tin thin films. Superlattices and Microstructures, 2008, 44, 641-649.	3.1	35
26	The critical role of didodecyldimethylammonium bromide on physico-chemical, technological and biological properties of NLC. Colloids and Surfaces B: Biointerfaces, 2014, 121, 1-10.	5.0	35
27	Synthesis and growth mechanism of dendritic Cu2â^'xSe microstructures. Journal of Alloys and Compounds, 2012, 538, 8-10.	5.5	34
28	Structural and electrical properties of In2O3/SeO2thin films for gas-sensing applications. Journal Physics D: Applied Physics, 2001, 34, 2097-2102.	2.8	33
29	Physical Properties of Molybdenum Oxide Thin Films for NO Gas Detection. Physica Status Solidi A, 1998, 168, 249-256.	1.7	32
30	Characterization and Growth Mechanism of Selenium Microtubes Synthesized by a Vapor Phase Deposition Route. Crystal Growth and Design, 2010, 10, 4890-4897.	3.0	32
31	Physical properties of sputtered molybdenum oxide thin films suitable for gas sensing applications. Journal Physics D: Applied Physics, 2002, 35, 228-233.	2.8	30
32	Copper and ceruloplasmin dyshomeostasis in serum and cerebrospinal fluid of multiple sclerosis subjects. Biochimica Et Biophysica Acta - Molecular Basis of Disease, 2018, 1864, 1828-1838.	3.8	30
33	Ferulic Acid-NLC with Lavandula Essential Oil: A Possible Strategy for Wound-Healing?. Nanomaterials, 2020, 10, 898.	4.1	30
34	Langmuir-Blodgett films of Cu(II)-tetrakis (3,3-dimethylbutoxycarbonyl) phthalocyanine: a spectrophotometric and TEM analysis of their structure and morphology. Thin Solid Films, 1996, 280, 249-255.	1.8	28
35	Innovative hybrid vs polymeric nanocapsules: The influence of the cationic lipid coating on the "4S― Colloids and Surfaces B: Biointerfaces, 2016, 141, 450-457.	5.0	28
36	Promising Piezoelectric Properties of New ZnO@Octadecylamine Adduct. Journal of Physical Chemistry C, 2015, 119, 20143-20149.	3.1	27

#	Article	IF	CITATIONS
37	Cyto/Biocompatibility of Dopamine Combined with the Antioxidant Grape Seed-Derived Polyphenol Compounds in Solid Lipid Nanoparticles. Molecules, 2021, 26, 916.	3.8	27
38	Growth of single-walled carbon nanotubes by a novel technique using nanosized graphite as carbon source. Chemical Physics Letters, 2000, 327, 284-290.	2.6	25
39	Synthesis and Characterization of TiO2Nanocrystals Prepared fromn-Octadecylamineâ^'Titanyl Oxalate Langmuirâ^'Blodgett Films. Langmuir, 2003, 19, 3486-3492.	3.5	23
40	Self-Assembly of n-Diamond Nanocrystals Into Supercrystals. Crystal Growth and Design, 2009, 9, 1245-1249.	3.0	23
41	Thermal deposition and characterization of Se-Sn mixed oxide thin films for NO gas sensing applications. Journal of Applied Physics, 1998, 83, 3541-3546.	2.5	22
42	Study of Gas Sensing Performances of Langmuirâ^'Blodgett Films Containinig an Alkyne-Linked Conjugated-Porphyrin Dimer. Langmuir, 2001, 17, 8139-8144.	3.5	22
43	Interaction of pH-sensitive non-phospholipid liposomes with cellular mimetic membranes. Biomedical Microdevices, 2013, 15, 299-309.	2.8	22
44	Investigations on graphene oxide for ion beam dosimetry applications. Vacuum, 2020, 178, 109451.	3.5	22
45	Optical absorption and structure of thermally annealed gallium selenide thin films. Journal of Applied Physics, 1989, 65, 1164-1167.	2.5	21
46	Monitoring prion protein expression in complex biological samples by SERS for diagnostic applications. Nanotechnology, 2010, 21, 165502.	2.6	21
47	Self-assembly and branching of sucrose stabilized silver nanoparticles by microwave assisted synthesis: From nanoparticles to branched nanowires structures. Colloids and Surfaces A: Physicochemical and Engineering Aspects, 2009, 348, 205-211.	4.7	20
48	Structural and spectroscopic investigations on graphene oxide foils irradiated by ion beams for dosimetry application. Vacuum, 2021, 188, 110185.	3.5	20
49	Correlation between the structural and optical properties of polydispersed II–VI quantum dots in glass matrix. Journal of Applied Physics, 1991, 70, 6898-6901.	2.5	19
50	Sputter deposition of tungsten trioxide for gas sensing applications. Journal of Materials Science: Materials in Electronics, 1998, 9, 317-322.	2.2	19
51	A silver nanoparticle-poly(methyl methacrylate) based colorimetric sensor for the detection of hydrogen peroxide. Heliyon, 2019, 5, e02887.	3.2	19
52	Organization of single-walled nanotubes into macro-sized rectangularly shaped ribbons. Chemical Physics Letters, 2003, 381, 86-93.	2.6	18
53	Colloidal solution of silver nanoparticles for label-free colorimetric sensing of ammonia in aqueous solutions. Beilstein Journal of Nanotechnology, 2018, 9, 499-507.	2.8	17
54	Electron diffraction study of melt-grown InSe crystals. Nuovo Cimento Della Societa Italiana Di Fisica D - Condensed Matter, Atomic, Molecular and Chemical Physics, Biophysics, 1986, 7, 795-806.	0.4	16

#	Article	IF	CITATIONS
55	LB multilayers of highly conjugated porphyrin dimers: differentiation of properties and behaviour between the free base and the metallated derivatives. Colloids and Surfaces A: Physicochemical and Engineering Aspects, 2002, 198-200, 897-904.	4.7	16
56	SERS based optical sensor to detect prion protein in neurodegenerate living cells. Sensors and Actuators B: Chemical, 2011, 156, 479-485.	7.8	16
57	A simple approach to synthetize folic acid decorated magnetite@SiO <sub>2</sub> nanostructures for hyperthermia applications. Journal of Materials Chemistry B, 2017, 5, 7547-7556.	5.8	16
58	Effect of temperature on the physical, optical and photocatalytic properties of TiO2 nanoparticles. SN Applied Sciences, 2020, 2, 1.	2.9	16
59	Convergent-beam electron diffraction study of melt-and vapour-grown single crystals of gallium chalcogenides. Nuovo Cimento Della Societa Italiana Di Fisica D - Condensed Matter, Atomic, Molecular and Chemical Physics, Biophysics, 1989, 11, 1145-1163.	0.4	15
60	Metalorganic vapour phase epitaxy growth of ZnS layers by (t-Bu)SH and Me2Zn:Et3N precursors. Journal of Crystal Growth, 1995, 156, 45-51.	1.5	15
61	Crossâ€sectional high resolution electron microscopy of Zn+ implanted and lowâ€power pulsedâ€laser annealed GaAs. Applied Physics Letters, 1996, 69, 4072-4074.	3.3	15
62	Meso- and nano-scale investigation of carbon fibers coated by nano-crystalline diamond. Chemical Physics Letters, 2005, 402, 340-345.	2.6	15
63	Photofunctional multilayer films by assembling naked silver nanoparticles and a tailored nitric oxide photodispenser at water/air interface. Journal of Colloid and Interface Science, 2012, 368, 191-196.	9.4	15
64	Synthesis and Characterization of Mixed Iron-Manganese Oxide Nanoparticles and Their Application for Efficient Nickel Ion Removal from Aqueous Samples. Journal of Analytical Methods in Chemistry, 2017, 2017, 1-9.	1.6	15
65	Enhanced adsorption capacity of porous titanium dioxide nanoparticles synthetized in alkaline sol. Applied Physics A: Materials Science and Processing, 2020, 126, 1.	2.3	15
66	Structural characterization of unhydrogenated amorphous GaAs. Journal of Non-Crystalline Solids, 1991, 127, 12-18.	3.1	14
67	Precipitation of superstructured nano-crystals in high-dose implanted Si: an XHRTEM study. Journal Physics D: Applied Physics, 2004, 37, 2730-2736.	2.8	14
68	Synthesis and <i>in vitro</i> Cytotoxicity of Glycans-Capped Silver Nanoparticles. Nanomaterials and Nanotechnology, 2011, 1, 10.	3.0	14
69	High ordered biomineralization induced by carbon nanoparticles in the sea urchin <i>Paracentrotus lividus</i> . Nanotechnology, 2012, 23, 495104.	2.6	14
70	Controlled synthesis and chain-like self-assembly of silver nanoparticles through tertiary amine. Colloids and Surfaces A: Physicochemical and Engineering Aspects, 2013, 417, 10-17.	4.7	14
71	From GO to rGO: An analysis of the progressive rippling induced by energetic ion irradiation. Applied Surface Science, 2022, 586, 152789.	6.1	14
72	Study of the polytypism in melt grown InSe single crystals by convergent beam electron diffraction. Journal of Crystal Growth, 1990, 100, 347-353.	1.5	13

#	Article	IF	CITATIONS
73	Surface structural and morphological characterization of ZnTe epilayers grown on {100} GaAs by MOVPE. Journal of Crystal Growth, 1993, 128, 633-638.	1.5	13
74	Physical characterization of In2Se3 thin films prepared by electron beam evaporation. Vacuum, 1995, 46, 997-1000.	3.5	13
75	Photoconductivity of Packed Homotype Bundles Formed by Aligned Single-Walled Carbon Nanotubes. Nano Letters, 2008, 8, 968-971.	9.1	13
76	Role of the Cellular Prion Protein in the Neuron Adaptation Strategy to Copper Deficiency. Cellular and Molecular Neurobiology, 2012, 32, 989-1001.	3.3	13
77	Silver and carbon nanoparticles toxicity in sea urchin Paracentrotus lividus embryos. BioNanoMaterials, 2013, 14, .	1.4	13
78	Cytotoxicity of $\hat{I}^2$ -D-glucose coated silver nanoparticles on human lymphocytes. AIP Conference Proceedings, 2014, , .	0.4	13
79	Synergistic Effect Induced by Gold Nanoparticles with Polyphenols Shell during Thermal Therapy: Macrophage Inflammatory Response and Cancer Cell Death Assessment. Cancers, 2021, 13, 3610.	3.7	13
80	Essential Oil-Loaded NLC for Potential Intranasal Administration. Pharmaceutics, 2021, 13, 1166.	4.5	13
81	Growth and characterization of tin oxide thin films prepared by reactive sputtering. Solar Energy Materials and Solar Cells, 1993, 31, 235-242.	6.2	12
82	Gas sensing properties of meso,meso′-buta-1,3-diyne-bridged Cu(II) octaethylporphyrin dimer Langmuir–Blodgett films. Sensors and Actuators B: Chemical, 1999, 57, 179-182.	7.8	12
83	High resolution transmission electron microscopy of elevated temperature Zn+ implanted and low-power pulsed laser annealed GaAs. Journal of Applied Physics, 2000, 88, 1806-1810.	2.5	12
84	Structural reordering and electrical activation of ion-implanted GaAs and InP due to laser annealing in a controlled atmosphere. Physical Review B, 1999, 59, 2986-2994.	3.2	11
85	Modulation of charge transport in diamond-based layers. Journal of Applied Physics, 2003, 94, 416-422.	2.5	11
86	Organized networks of helically wound single-walled C-nanotubes. Chemical Physics Letters, 2004, 388, 36-39.	2.6	11
87	Assembly of hybrid silver–titania thin films for gas sensors. Sensors and Actuators B: Chemical, 2010, 145, 794-799.	7.8	11
88	Shape-dependent plasmon resonances of Ag nanostructures. Superlattices and Microstructures, 2010, 47, 66-71.	3.1	11
89	Solid-to-solid phase transformations of nanostructured selenium-tin thin films induced by thermal annealing in oxygen atmosphere. , 2014, , .		11
90	Morphological, structural and electrical characterization of nanostructured vanadium–tin mixed oxide thin films. Journal of Non-Crystalline Solids, 2004, 341, 68-76.	3.1	10

#	Article	IF	CITATIONS
91	Langmuir-Blodgett films of a phthalocyanine symmetrically functionalized with eight ester units. Materials Science and Engineering C, 1998, 5, 317-320.	7.3	9
92	Characterization of ablation plasma ion implantation. Nuclear Instruments & Methods in Physics Research B, 2005, 240, 36-39.	1.4	9
93	Self-assembling of micro-patterned titanium oxide films for gas sensors. Sensors and Actuators B: Chemical, 2009, 140, 563-567.	7.8	9
94	Nanographite assembled films for sensitive NO2 detection. Sensors and Actuators B: Chemical, 2012, 161, 359-365.	7.8	9
95	Copper Dependent Modulation of α-Synuclein Phosphorylation in Differentiated SHSY5Y Neuroblastoma Cells. International Journal of Molecular Sciences, 2021, 22, 2038.	4.1	9
96	Stress response induced by carbon nanoparticles in Paracentrotus lividus. International Journal of Molecular and Cellular Medicine, 2012, 1, 30-8.	1.1	9
97	Solid Lipid Nanoparticles Administering Antioxidant Grape Seed-Derived Polyphenol Compounds: A Potential Application in Aquaculture. Molecules, 2022, 27, 344.	3.8	9
98	Gas-sensing properties of multilayers of two new macrocyclic copper complexes. Sensors and Actuators B: Chemical, 1997, 44, 585-589.	7.8	8
99	Thermal deposition and characterisation of In–Se mixed oxides thin films for NO gas sensing applications. Sensors and Actuators B: Chemical, 1999, 58, 356-359.	7.8	8
100	Calcite-forming <i>Bacillus licheniformis</i> Thriving on Underwater Speleothems of a Hydrothermal Cave. Geomicrobiology Journal, 2018, 35, 804-817.	2.0	8
101	Structural phase modifications induced by energetic ion beams in graphene oxide. Vacuum, 2021, 193, 110513.	3.5	7
102	Green Silver Nanoparticles Promote Inflammation Shutdown in Human Leukemic Monocytes. Materials, 2022, 15, 775.	2.9	7
103	Temperature-dependent conduction of W-containing composite diamond films. Applied Physics Letters, 2001, 79, 2007-2009.	3.3	6
104	Optical, morphological and structural characterization of Langmuir–Schaefer films of a functionalized copper phthalocyanine. Journal of Colloid and Interface Science, 2011, 363, 199-205.	9.4	6
105	Nondestructive Analysis of Silver Coins Minted in Taras (South Italy) between the V and the III Centuries BC. Journal of Archaeology, 2014, 2014, 1-12.	0.5	6
106	TiO 2 films by solâ€gel spinâ€coating deposition with microbial antiadhesion properties. Surface and Interface Analysis, 2019, 51, 1351-1358.	1.8	6
107	Structural characterization of hydrogenated amorphous GaAs. Journal of Non-Crystalline Solids, 1992, 151, 253-260.	3.1	5
108	Structural and morphological analysis of reactively sputtered tellurium suboxide thin films. Journal of Non-Crystalline Solids, 1993, 155, 67-76.	3.1	5

#	Article	IF	CITATIONS
109	Ion-Beam-Assisted Nanocrystal Formation in Silicon Implanted with High Doses of Pb+and Bi+Ions. Japanese Journal of Applied Physics, 2001, 40, 5841-5849.	1.5	5
110	Single step synthesis of SnO2–SiO2 core–shell microcables. Journal of Crystal Growth, 2011, 330, 22-29.	1.5	5
111	Aligned selenium microtubes array: Synthesis, growth mechanism and photoelectrical properties. Chemical Physics Letters, 2011, 510, 87-92.	2.6	5
112	Highly sensitive conformational switching of ethane-bridged mono-zinc bis-porphyrin as an application tool for rapid monitoring of aqueous ammonia and acetone. Sensors and Actuators B: Chemical, 2018, 257, 685-691.	7.8	5
113	Wavelength, fluence and substrate-dependent room temperature pulsed laser deposited B-enriched thick films. Applied Surface Science, 2019, 483, 1044-1051.	6.1	5
114	Magnetostatic Field System for Uniform Cell Cultures Exposure. PLoS ONE, 2013, 8, e72341.	2.5	5
115	Proton beam dosimetry based on the graphene oxide reduction and Raman spectroscopy. Vacuum, 2022, 201, 111113.	3.5	5
116	Convergent-beam electron diffraction analysis of GaSe crystals grown from the melt by different doping elements. Nuovo Cimento Della Societa Italiana Di Fisica D - Condensed Matter, Atomic, Molecular and Chemical Physics, Biophysics, 1991, 13, 233-245.	0.4	4
117	Analysis of nuclear transmutations observed in D- and H-loaded Pd films. International Journal of Hydrogen Energy, 2002, 27, 527-531.	7.1	4
118	High Doses of Silica Nanoparticles Obtained by Microemulsion and Green Routes Compromise Human Alveolar Cells Morphology and Stiffness Differently. Bioinorganic Chemistry and Applications, 2022, 2022, 1-23.	4.1	4
119	Numerical evaluation of lattice parameters from high-order Laue zone lines in convergent-beam electron diffraction disks. Ultramicroscopy, 1988, 26, 377-384.	1.9	3
120	Convergent-beam electron diffraction characterization of dislocations in GaS single crystals. Ultramicroscopy, 1990, 33, 143-149.	1.9	3
121	Comparative optical and morphological investigation of meso,meso′-buta-1,3-diyne-bridged Cu(II) octaethyl porphyrin dimer Langmuir–Blodgett films. Materials Science and Engineering C, 1999, 8-9, 107-111.	7.3	3
122	Unusual coin from the Parabita hoard: combined use of surface and micro-analytical techniques for its characterisation. Journal of Cultural Heritage, 2010, 11, 233-238.	3.3	3
123	Characterization of Composite Phthalocyanine–Fatty Acid Films from the Air/Water Interface to Solid Supports. Journal of Physical Chemistry B, 2011, 115, 14956-14962.	2.6	3
124	Electronic properties of individual and assembled homotype SWCNT bundles. Chemical Physics Letters, 2011, 509, 152-157.	2.6	3
125	The tale of Henry VII: a multidisciplinary approach to determining the post-mortem practice. Archaeological and Anthropological Sciences, 2017, 9, 1215-1222.	1.8	3
126	Design and Synthesis of Ironâ€Đoped Nanostructured TiO <sub>2</sub> and Its Potential Use in the Photodegration of Hazardous Materials Present in Personal Care Products. ChemistrySelect, 2017, 2, 5095-5099.	1.5	3

#	Article	IF	CITATIONS
127	Photochromic properties in silver-doped titania nanoparticles. Materials Research Express, 2019, 6, 036206.	1.6	3
128	Tailoring sheet resistance through laser fluence and study of the critical impact of a V-shaped plasma plume on the properties of PLD-deposited DLC films for micro-pattern gaseous detector applications. Diamond and Related Materials, 2022, 124, 108909.	3.9	3
129	Electron diffraction study of In2Se3 melt grown crystals. Journal of Crystal Growth, 1989, 96, 947-952.	1.5	2
130	Convergent beam electron diffraction study of extended defects in gallium chalcogenide single crystals grown from the melt. Semiconductor Science and Technology, 1992, 7, A122-A126.	2.0	2
131	Physical Properties of Molybdenum Oxide Thin Films for NO Gas Detection. Physica Status Solidi A, 1998, 168, 249-256.	1.7	2
132	Thermal neutron conversion by high purity 10B-enriched layers: PLD-growth, thickness-dependence and neutron-detection performances. European Physical Journal Plus, 2022, 137, 1.	2.6	2
133	<title>Optical investigation of microcrystals in glasses</title> . , 1991, 1513, 130.		1
134	Analysis of extended defects in melt-grown GaSe single crystals by convergent-beam electron diffraction techniques. Ultramicroscopy, 1991, 35, 71-76.	1.9	1
135	Characterization of CdS epitaxial films by high energy reflected electrons. Journal of Crystal Growth, 1990, 101, 185-189.	1.5	Ο
136	Temperature and ion flux dependence of damage structures in Zn+ implanted and laser annealed GaAs. Journal Physics D: Applied Physics, 2002, 35, 2830-2836.	2.8	0
137	High-resolution electron microscopy of Zn- and Bi-related superlattices in ion implanted (1 0 0) Si. Journal of Materials Science: Materials in Electronics, 2003, 14, 783-786.	2.2	0
138	Characterization of Pd-H/sub 2/ thin films irradiated by UV laser. , 0, , .		0
139	Effects of hydrogen diffusion and UV irradiation in Pd thin films. , 2003, , .		Ο
140	<title>Performance study of hydrogen effect in Pd thin films irradiated by a UV irradiation</title> . , 2003, 5147, 185.		0
141	Iris revolutaColas., natural hybrid origin species: characterization and preservation problems. Plant Biosystems, 2008, 142, 162-165.	1.6	Ο
142	Nanoclustering in Silicon Induced by Oxygen Ions Implanted. Nanomaterials and Nanotechnology, 2011, 1, 16.	3.0	0
143	Plasmonic Light Trapping in Titania–Silver Dots Thin Films. Physica Status Solidi (B): Basic Research, 2020, 257, 2070035.	1.5	0
144	Plasmonic Light Trapping in Titania–Silver Dots Thin Films. Physica Status Solidi (B): Basic Research, 2020, 257, 2000124.	1.5	0

#	Article	IF	CITATIONS
145	Surface architecture of Neisseria meningitidis capsule and outer membrane as revealed by atomic force microscopy. Research in Microbiology, 2021, 172, 103865.	2.1	0
146	CBED analysis of extended defects in melt-grown GaSe single crystals. Proceedings Annual Meeting Electron Microscopy Society of America, 1990, 48, 494-495.	0.0	0
147	A Comparative Study of Pottery from Mersin-Yumuktepe and Arslantepe, Turkey. Archaeological Discovery, 2015, 03, 15-25.	0.5	0
148	Hydrogen peroxide LSPR sensing with unoxidised CuNPs-Tween® 60. Journal of Materials Science, 2022, 57, 1714.	3.7	0